Probing hydrogen positions in hydrous compounds: information from parametric neutron powder diffraction studies †

Valeska P. Ting[a], Paul F. Henry[b], Marc Schmidtmann[c], Chick C. Wilson[d] and Mark T. Weller[*a]

Received (in XXX, XXX) Xth XXXXXXXXX 200X, Accepted Xth XXXXXXXXX 200X
First published on the web Xth XXXXXXXXX 200X
DOI: 10.1039/b000000x

We demonstrate the extent to which modern detector technology, coupled with a high flux constant wavelength neutron source, can be used to obtain high quality diffraction data from short data collections, allowing the refinement of the full structures (including hydrogen positions) of hydrous compounds from *in situ* neutron powder diffraction measurements. The *in situ* thermodiffractometry and controlled humidity studies reported here reveal that important information on the reorientations of structural water molecules with changing conditions can be easily extracted, providing insight into the effects of hydrogen bonding on bulk physical properties. Using crystalline $BaCl_2.2H_2O$ as an example system, we analyse the structural changes in the compound and its dehydration intermediates with changing temperature and humidity levels to demonstrate the quality of the dynamic structural information on the hydrogen atoms and associated hydrogen bonding that can be obtained without resorting to sample deuteration.

Introduction

Parametric powder diffraction studies provide information on structural changes as a function of a variable, most commonly temperature or time under set conditions of *e.g.* humidity. Powder thermodiffractometry, using either X-ray or neutron scattering, is a technique that has been widely applied to the study of decomposition and transformation routes in solids [1-4], impacting on such practical problems as storage of anhydrous pharmaceuticals, wetting/curing of building materials, such as gypsum and cements, and the use of industrial desiccants, for example anhydrous salts and zeolites. Powder thermodiffractometry is primarily used to collect basic information on phase behaviour during such processes *via* quantitative phase analysis, which involves comparing the ratios of integrated intensities (*e.g.* during "curing" of hydrous building materials[5]), or to track changes in unit cell parameters as a function of temperature (for example, during the dehydration of zeolitic materials [6] or in the study of materials displaying negative thermal expansion[7]). It is less common for profile fitting methods, which allow structural parameters such as site occupancies and atomic positions to be determined as a function of temperature, to be used to obtain detailed structural information from variable temperature diffraction profiles. When performed, such structural thermodiffractometry studies will chiefly focus on changes in heavy atom positions (typically *via* X-ray diffraction [8, 9]) or oxygen positions (using neutron diffraction [10, 11]), while the changes in hydrogen positions in inorganic compounds during thermal decompositions are generally not taken into account. As many thermal decomposition reactions of importance involve hydrogen-containing species, in particular, the water molecules of hydrated compounds, the extent of hydrogen bonding present in hydrous species can greatly contribute to the stability of a particular crystalline form. For example, the decomposition of salt hydrates, hydrated zeolite/zeolite-related framework structures and of clays all involve the loss of water, often *via* formation of intermediate partially hydrated phases [5, 12], and having information on the hydrogen bonding in these structures would greatly enhance understanding of the mechanisms of the transformations.

While the short data collection times necessary for temperature or time resolution in *in situ* parametric studies is provided by X-ray diffraction (XRD), the technique's insensitivity to light atoms (such as H) in the presence of heavier metals means that hydrogen positions from XRD are rarely directly refined. Neutron powder diffraction (NPD) has many practical advantages for hydrogenous materials, which include superior resolution of the positions of light atoms in the presence of heavier Z elements (*c.f.* X-ray diffraction), and the capability to handle large sample sizes, which provides information on the bulk sample and the ability to track changes that involve significant changes in unit cell dimensions or sample density (an important advantage over single crystal studies, where there is the risk of the single crystal shattering at phase boundaries).

The large incoherent neutron scattering background of the ^1H isotope is typically combated in static neutron diffraction experiments by employing sample deuteration. Sample deuteration, however, complicates parametric measurements to a much greater extent than it does static, ex-situ structural characterisation, as the practicalities of handling and continuously measuring deuterated samples under changing conditions while keeping them in closed environments to prevent isotopic exchange are non-trivial and preclude dynamic analysis of deuterated materials in a standard furnace. Furthermore, structural differences that occur as a result of isotope effects are well documented [13-15].Therefore, the aquisition of high-quality data from non-deuterated samples would be vastly preferable.

As has been detailed in recent publications [16] the latest generation of high-flux fixed-wavelength neutron instruments with improved detector stability are exceptionally well-suited to the study of polycrystalline hydrogenous materials in their native (non-deuterated) form using NPD. The recent improvements in detector stability can be attributed to the greater stability of ^{3}He microstrip detectors [17] (such as those used on D20 at the Insitut Laue Langevin, (ILL)) with respect to time, combined with the capability of such detectors to handle high count rates. The detector stability (which, in the case of D20, is enhanced by extensive outgassing of the detectors, ensuring purity of the work gas) results in more uniform detector efficiencies, compared to, for example, stretched wire detectors, while the high count rates allow optimisation of peak to background ratios[18]. Both aspects, together with a well-defined peak shape and good $\Delta d/d$ resolution, allow the large incoherent scattering background of ^{1}H to be reliably fitted using a smooth function and subtracted from the data, meaning that structural refinements of hydrogen-containing samples can be performed without the need for sample deuteration.

In order to critically assess the quality of the crystallographic information on hydrogen positions that can be extracted from parametric studies using high-resolution NPD data, the simple salt hydrate $BaCl_2.2H_2O$ and its dehydration products were used as example compounds for *in situ* dehydration and hydration experiments, concentrating in particular on the positions and orientations of the hydrogen atoms comprising the water molecules. The crystal structures of the dihydrate and of the intermediate monohydrate material had been previously studied at static temperatures by single crystal neutron diffraction (SND) by Padmanabhan *et al.* [19] and single crystal X-ray diffraction (SXD) by Lutz *et al.* [20], and were assigned space groups $P2_1/c$ and *Pnma*, respectively. The SXD study of the heavy metal chloride monohydrate resulted in poorly defined hydrogen positions, suffering from errors (such as unrealistically short O-H bond distances) associated with determination of electron densities rather than nuclear positions. The structure was subsequently improved by Moller *et al.* [21], using NPD on the deuterated analogue of the monohydrate material to determine probable positions for the deuterium atoms.

In this work, the changes in the structure of the intermediate compound and the transformations between the different hydrated forms of $BaCl_2$ were studied directly using *in situ* dehydration of the hydrogenous dihydrate material using neutron powder diffraction. In addition, the structure of the intermediate monohydrate compound, as refined against data from the dehydration of the dihydrate and hydration of the anhydrous $BaCl_2$ is fully analysed for comparison.

Experimental

A sample of polycrystalline $BaCl_2.2H_2O$ (99%) was used as-received from Sigma Aldrich. Thermogravimetric analysis (TGA) was run on a ~20 mg sample of $BaCl_2.2H_2O$ over the temperature range room temperature (RT) to 400°C at a heating rate of 5 °C.min^{-1}. The NPD measurements were collected on the D20 diffractometer at the ILL[22], operating in its high take-off angle configuration at a fixed wavelength of 1.87 Å. The *in situ* dehydration was performed using the standard furnace ancillary, from RT to approximately 160°C. A 5 g sample of polycrystalline $BaCl_2.2H_2O$ was placed in the bulb of a long-necked silica tube left open to the atmosphere at the neck end to allow for evaporation of water. An initial data set was collected at RT for 30 minutes and the sample was then ramped at 1.5 °C.min^{-1} to ~160 °C with continuous data collection binned into a series of five minute (~7.5 °C temperature range) sets, to produce 32 good quality data sets. For the *in situ* hydration experiments, anhydrous $BaCl_2$ was prepared by heating $BaCl_2.2H_2O$ at 400 °C under vacuum. NPD data was collected over a 12 hr period during the dynamic hydration of a 3 g sample of the $BaCl_2$ powder suspended in a heavily perforated vanadium sample can in a humid flow of N_2 gas at 100% relative humidity (RH) at 298 K. The sample was exposed to water vapour during a 10 minute equilibration interval prior to collection of the first diffraction profile, and full NPD patterns were collected over consecutive 2.5 min intervals thereafter. The resultant powder diffraction patterns were analysed *via* Rietveld refinement using the GSAS [23] Rietveld refinement program in conjunction with the EXPGUI [24] user interface.

3. Results and Discussion

3.1 Dehydration of $BaCl_2.2H_2O$ and initial refinement of the static phases

In order to track the transformations between the different decomposition products of $BaCl_2.2H_2O$ with time, the structures of these phases as well as the temperature ranges over which each phase was present needed to be established. Thermogravimetric analysis of $BaCl_2.2H_2O$ showed a weight loss resulting in the formation of the monohydrate near 80 °C, and a further decomposition to the anhydrous form at ~120 °C, indicating that the monohydrate intermediate was the stable phase between these two temperatures.

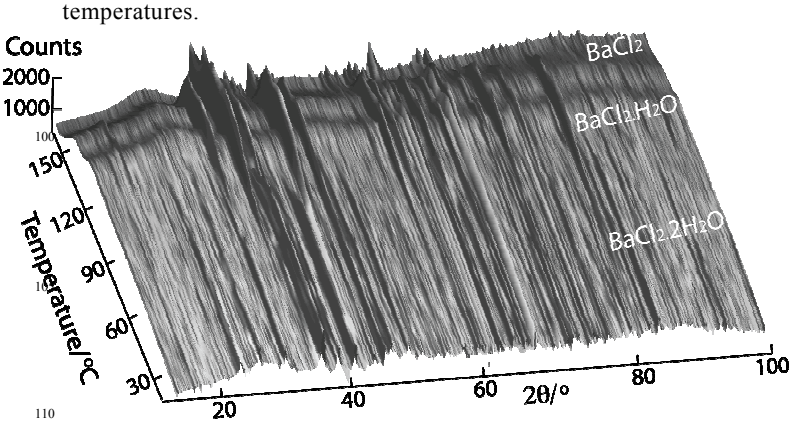

Figure 1. NPD thermodiffractogram showing the Bragg peaks relating to the $BaCl_2.2H_2O$ phase being replaced by those relating to the intermediate $BaCl_2.H_2O$ phase, and the anhydrous $BaCl_2$ phase upon heating.

The thermodiffractogram derived from this data collection, presented in Figure 1, shows the Bragg peaks corresponding to the $BaCl_2.2H_2O$ phase at RT being replaced by those relating to the intermediate $BaCl_2.H_2O$ phase at ~85 °C, and finally by the anhydrous $BaCl_2$ phase at ~130 °C, in agreement with the TGA results.

The existence of the two-phase regions necessitated the use of good starting models for each of the three phases of interest. The initial 30 min RT data set of $BaCl_2.2H_2O$ was refined using the literature model derived from the SND study of Padmanabhan *et al*. (1978) as a starting model. A 10-parameter polynomial fit was used to model the high, complex background associated with the incoherent scattering contribution from hydrogen and the contributions from the silica sample tube. The Rietveld refinement of the model proceeded smoothly with no constraints on positional or isotropic atomic displacement parameters (ADPs), and converged with a χ^2= 1.652 and RF^2 = 9.2 %.

Final crystallographic data are summarized in Table 1 and the final background-subtracted profile fit is shown in Figure 2. Derived positional parameters were in accordance with the SND study, with the refined hydrogen–oxygen distances reflecting true inter-nuclear separations: O1_H1 = 0.96(3) Å, O1_H2 = 0.94(2) Å, O2_H3 = 0.92(2) Å, O2_H4 = 0.90(3) Å, with H1_O1_H2 = 101.5(17)° and H3_O2_H4 = 101.4(17)°.

Above ~100 °C the diffraction patterns that were collected under heating could be fitted using a single phase ($BaCl_2.H_2O$) until ~125 °C when peaks relating to the anhydrous $BaCl_2$ phase began to appear.

Table 1: Refined atomic coordinates and isotropic thermal parameters (Ui/Ue) for $BaCl_2.2H_2O$ at RT (30 min data collection) at a wavelength of 1.87 Å; $P2_1/n$, a = 6.7265(7) Å, b = 10.9141(10) Å, c = 7.1358(7) Å, β= 91.096(4)°, V = 523.77(9) Å^3, χ2= 1.652, RF^2 = 9.2% . Occupancies of all atoms = 1. All atoms have 4e site symmetry.

Atom	x	y	z	Ui/Ue*100 / Å^2
Ba1	0.5434(15)	0.2811(9)	0.6434(13)	1.3(3)
Cl1	0.8643(8)	0.0808(5)	0.7945(7)	2.16(18)
Cl2	0.6401(8)	0.1061(5)	0.3021(8)	1.74(18)
O1	0.3776(13)	0.1414(10)	0.9416(13)	1.5(2)
O2	0.2026(13)	0.1462(10)	0.5052(13)	1.6(2)
H1	0.357(3)	0.0616(21)	0.889(3)	5.5(6)
H2	0.472(3)	0.1249(17)	0.037(2)	4.3(5)
H3	0.104(2)	0.1367(15)	0.592(2)	4.0(4)
H4	0.236(3)	0.0677(20)	0.483(3)	5.0(5)

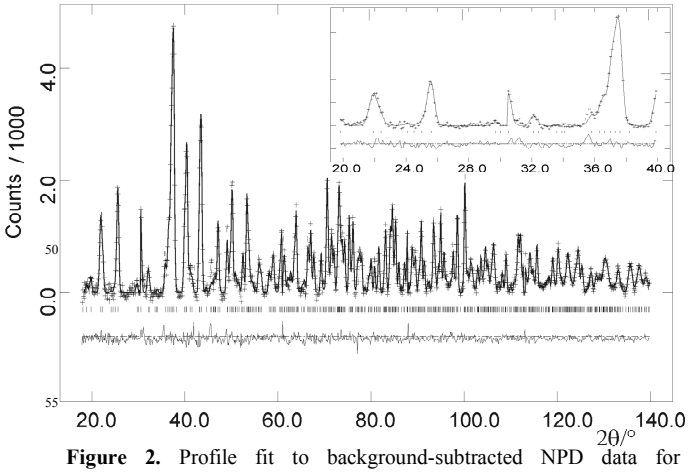

Figure 2. Profile fit to background-subtracted NPD data for $BaCl_2.2H_2O$ at RT (30 min data collection), showing the data, profile fit, tick markers for peak positions and difference profile. Inset 20-40° region expanded.

As an example of how thermodiffractometry can be used to investigate the structures of possibly transient intermediate phases, a data set with improved counting statistics for the intermediate $BaCl_2.H_2O$ phase was created by combining four data sets from the temperature range 100 – 120 °C, and the structure of the intermediate was refined against this longer data set, using the structure determined by Moller (1993) for $BaCl_2.2D_2O$ as a starting model. The refined atomic coordinates for $BaCl_2.H_2O$ at 110 ± 10 °C are given in Table 2, with anisotropic atomic displacement parameters (ADPs) in Table 3, and the final background-subtracted profile fit shown in Figure 3.

Table 2: Refined atomic coordinates and isotropic thermal parameters for $BaCl_2.H_2O$ at T = 110 ± 10 °C (20 min data collection) at a wavelength of 1.87 Å; *Pnma*, a = 11.1227(4) Å, b = 4.51108(15) Å, c = 9.0699(3) Å, V = 455.08(3) Å^3, χ2= 0.7392 , RF^2 = 7.96 %. All atoms have 4c site symmetry.

Atom	x	y	z	Ui/Ue*100 / Å^2
Ba1	0.1883(6)	0.25	0.1087(10)	2.02(16)
Cl1	0.1018(4)	0.75	-0.1179(7)	2.83(14)
Cl2	0.1233(4)	0.75	0.3358(5)	2.40(14)
O1	0.3457(7)	0.75	0.1032(13)	2.69(18)
H1	0.4081(15)	0.75	0.1620(21)	7.49*
H2	0.3910(18)	0.75	0.0109(16)	9.67

Table 3: Refined anisotropic ADPs (/Å^2) for hydrogen sites in $BaCl_2.H_2O$ at a wavelength of 1.87 Å.

Atom	U11*100/ Å^2	U22*100/ Å^2	U33*100/ Å^2	U12*100/ Å^2	U13*100/ Å^2	U23*100/ Å^2
H1	6.9(12)	5.6(8)	9.9(16)	0.00	-4.6(11)	0.00
H2	8.4(14)	14.0(15)	6.7(12)	0.00	5.5(11)	0.00

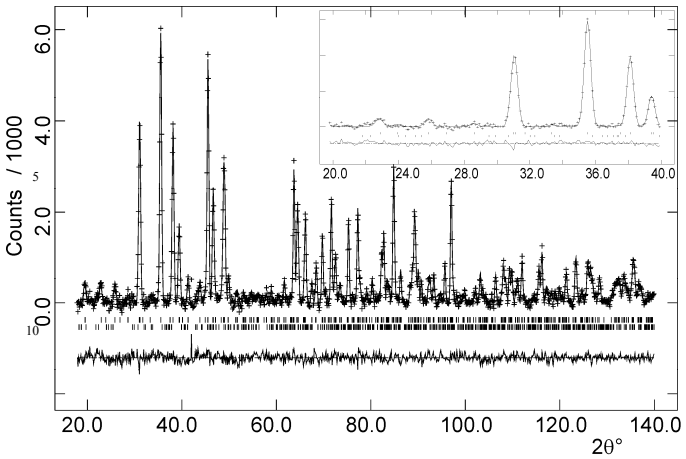

Figure 3. Profile fit to background-subtracted NPD data from $BaCl_2.H_2O$ for the temperature range T = 110 ± 10 °C (20 min data collection) showing the data, profile fit, tick markers for peak positions and difference profile. Inset 20-40° region expanded.

The structural model obtained is a clear improvement on that of Lutz in that the water molecule is more accurately defined (despite the higher temperature of data collection) with an O1_H1 distance of 0.88(2) Å, O1_H2 distance of 0.98(2) Å and H1_O1_H2 angle of 96.5(13)° (compared to distances of ~0.67 Å and 0.78 Å and an angle of 119.8° in Lutz *et al*.). Furthermore, Lutz's work had proposed the existence of an unusually symmetric bifurcated bond in order to explain the anomalous positive temperature shift of the OH stretching mode in IR/Raman spectra of $BaCl_2.H_2O$; as the H2 atom was very close to being in the O-Cl2 – Cl2 plane, it was asserted that thermal motion, which serves to straighten and strengthen typical "bent" bifurcated H-bonds, would have the effect of weakening the H2…Cl2 bond, since the H2 atom was very nearly in the O-Cl2-Cl2 plane. This was called into question by the subsequent study of the deuterated system (Moller *et al*, 1993), which showed the spectroscopic bands to be consistent with the existence of a single bifurcated and a single almost linear H bond

The geometry and orientation of the coordinated water molecule from this study were comparable with the structure refined by Moller *et al*. from NPD data on the deuterated analogue of the monohydrate material, undertaken at 295 K and 1.5 K, in that the hydrogen bonding scheme consisted of one bifurcated (H2 – Cl2) and one almost linear O – H….Cl hydrogen bond (H1 – Cl2), as opposed to the two sets of bifurcated bonds suggested by Lutz from analysis of refined X-ray O…Cl bond distances. Indeed, further refinement of the structure of $BaCl_2.H_2O$ at 110 ± 10 °C, incorporating anisotropic ADPs for the H atoms, suggested a water molecule with hydrogen thermal ellipsoids which were elongated to extend above and below the plane created by the Cl atoms (see Figure 4), on an angle which could reduce the length of the bifurcated H2…Cl2 bonds with increased thermal motion, contrary to the early model proposed by Lutz.

The monohydrate starting model that had been refined against the compiled data set at 110 ± 10 °C was used for dual phase profile fitting of the remaining NPD data sets (containing mixtures of the monohydrate and the anhydrous phase) over the temperature range 125-150 °C. The data at temperatures above 150 °C showed evidence of pure anhydrous $BaCl_2$, and the profile could be fitted using the crystallographic model of Brackett *et al*.[25] The final crystallographic description for $BaCl_2$, refined from a single data set, is presented in Table 4.

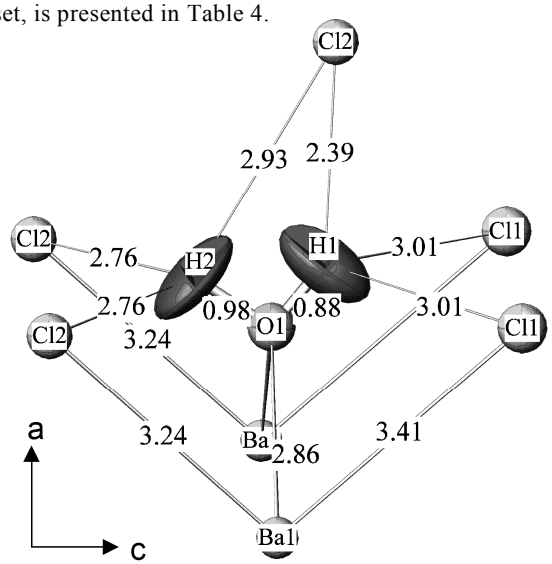

Figure 4. The structural model for $BaCl_2.H_2O$ (refined with anisotropic ADPs for the H atoms) showing bond lengths, as refined from the complied NPD data at T = 110 ± 10 °C (total 20 min data collection). The uncertainties in the quoted bond lengths (in Å) are between 0.01 and 0.02 Å

Table 4. Refined atomic coordinates and isotropic thermal parameters for anhydrous $BaCl_2$ from a 5 min data collection at T = 240 °C at a wavelength of 1.87 Å; *Pnma*, *a* = 7.9693(3) Å, *b* = 4.7931(2) Å, *c* = 9.4922(4)Å ; V = 362.58(3)Å^3, $\chi 2$= 0.738 , RF^2 = 7.88% . All atoms have 4c site symmetry.

Atom	x	y	z	Ui/Ue*100 / Å^2
Ba	0.2502(6)	0.25	0.1164(4)	3.53(14)
Cl1	0.1447(3)	0.25	0.4286(3)	4.71(8)
Cl2	0.0269(3)	0.25	0.8287(2)	5.60(10)

3.2 Evolution of the structures of $BaCl_2.2H_2O$, $BaCl_2.H_2O$ and $BaCl_2$ with temperature

In order to investigate the changes in the refined structures with temperature, the 32 five-minute thermodiffractometry data sets, starting with a data set centred on 37 °C, were analysed using the crystallographic starting models refined above. The SEQGSAS routine in the GSAS program was used to refine this model against successive data sets until a deterioration of fit parameters (corresponding to the formation of the monohydrate as a second phase contributing to the diffraction profile) was observed. At this point the monohydrate model was introduced into the profile fitting process and a dual phase refinement undertaken.

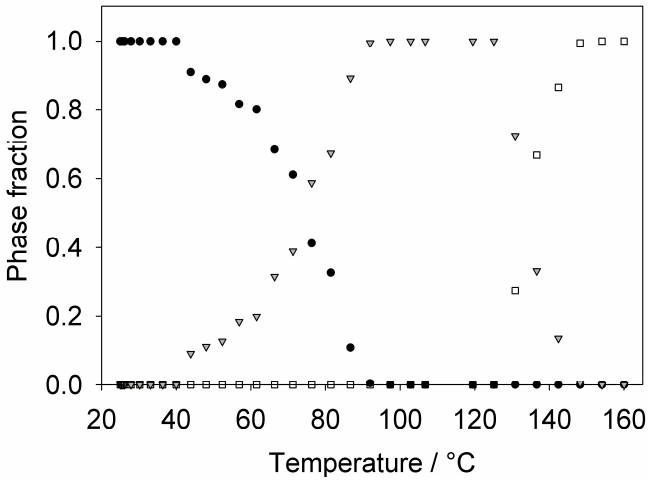

Figure 5. Refined phase fractions, as refined from the short NPD data collections, showing the $BaCl_2.2H_2O$ phase (black circles) being replaced by the intermediate $BaCl_2.H_2O$ phase (grey inverted triangles), which is in turn replaced by the anhydrous $BaCl_2$ phase (open squares) upon heating from RT to ~170 °C.

Full structural refinements including hydrogen positional parameters and isotropic ADPs were carried out where a contributing phase had a phase fraction of greater than 10 %, (*i.e* for the dihydrate, monohydrate and anhydrous phases, structural data could be extracted from the approximate temperature ranges RT – 80 °C, 50 – 145 °C and 135 –160 °C, respectively). At the point where a phase contributed only weakly to the profile intensity (less than ~10% of the intensity of the main reflections) only phase fractions and the profile parameters were refined for the relevant phase. Contributing phase fractions were extracted from the profile refinements and are summarised as a function of collection temperature in Figure 5.

To demonstrate the type of information that can be gained from full structural refinement of hydrogenous crystalline phases, the expansion of the monoclinic unit cell of $BaCl_2.2H_2O$ with temperature up to its decomposition was monitored *via* the evolution of its lattice parameters between RT and 80 °C (Figure 6). It was observed that expansion along the *a* and *c* axes is approximately twice as fast as along *b*. Of note is that there is no Ba-O bond along the *b* direction, only longer Ba-Cl and H---Cl interactions (see Figure 7).

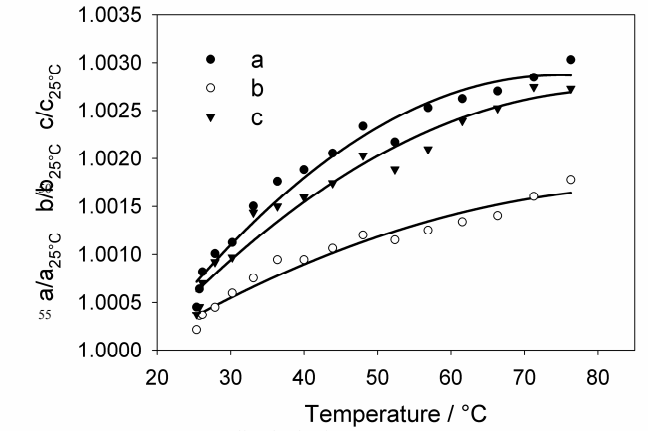

Figure 6. Normalised lattice parameters vs. temperature for $BaCl_2.2H_2O$ refined from the five-minute NPD data sets, showing the rate of expansion along each axis. The solid lines show regression fits to the data; error bars are within marker size.

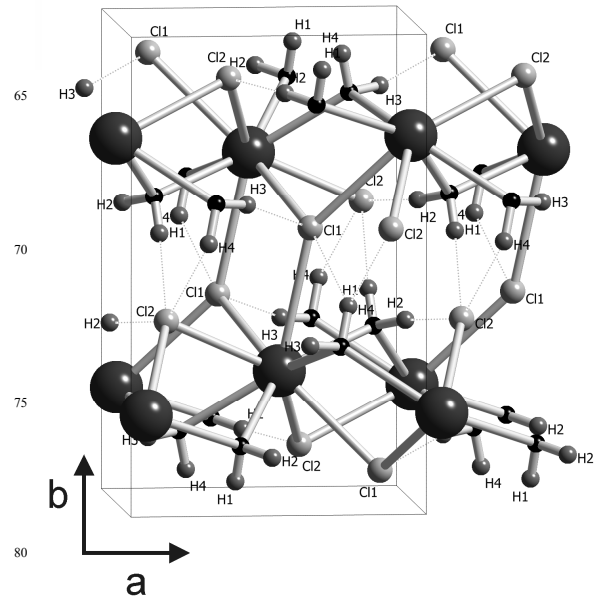

Figure 7. Structure of $BaCl_2.2H_2O$ refined from the 30 min NPD data set at RT. The large dark spheres are Ba atoms, the smaller dark spheres are the H_2O oxygen atoms.

In order to investigate this behaviour in more detail it was necessary to gain more information on the hydrogen positions and hydrogen bonding in the structure. Of the four hydrogen atoms, three (H1, H2 and H3 in Table 1) form strong, linear hydrogen bonds to chloride ions with Cl-H distances between 2.20(2) and 2.28(2) Å at room temperature. H4, however, forms bifurcated hydrogen bonds to Cl1 and Cl2 which, naturally, are significantly longer (between 2.57(2) and 2.64(2) Å), as can be seen in Figure 8. While the refined metal-anion distances and oxygen-hydrogen bond lengths vary smoothly as a function of temperature, increasing monotonically, the hydrogen bonding displays more complex behaviour with temperature. Upon heating, the linear hydrogen bonds elongate in accordance with the overall thermal expansion of the material and as these three bonds are directed along mainly the *a* and *c* directions, this is reflected in the lattice parameter changes.

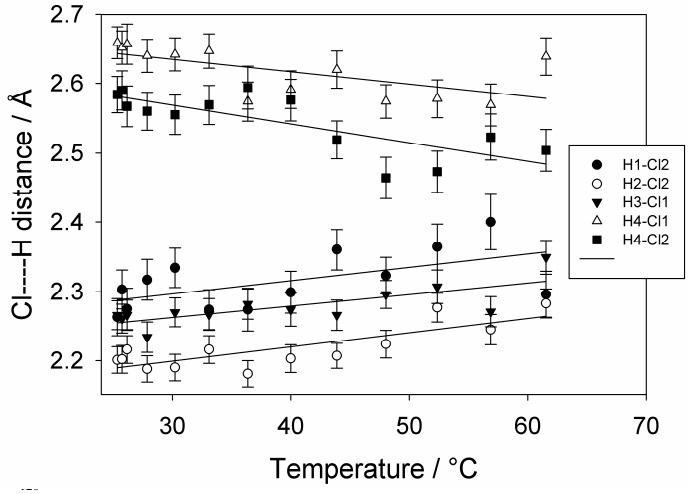

Figure 8. Variation of Cl…H hydrogen bonding distances in $BaCl_2.2H_2O$ with increased temperature, as refined from the five-minute NPD data sets. The solid lines show regression fits; error bars are shown.

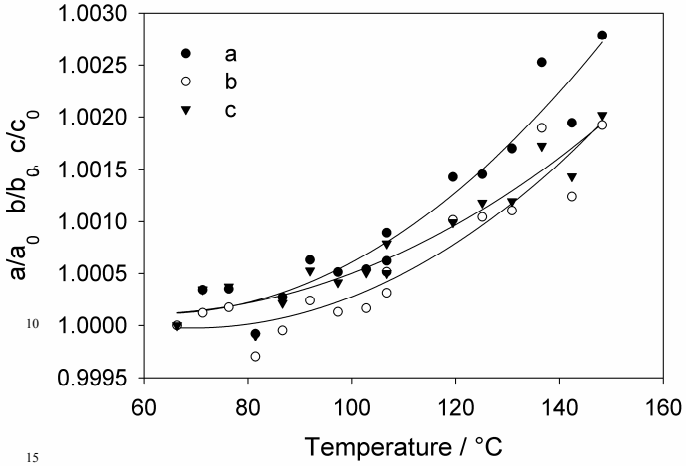

Figure 9. Normalised lattice parameters vs. temperature for $BaCl_2.H_2O$ refined from the five-minute NPD data sets. The solid lines show regression fits to the data; error bars are within the marker size. a_0, b_0 and c_0 refer to values at 67°C

The bifurcated hydrogen bonds, which lie mainly along the *b* axial direction, have bond strengths proportional to the combined strength of the hydrogen bonds to both acceptor groups [21], and are therefore stronger than the linear hydrogen bonds, despite having longer H…Cl distances. With increased temperature, these bonds prompt a minor reorientation of the water molecules, resulting in a slight shortening of their H…Cl distances and making the expansion along this axial direction much lower than in the other two directions.

Changes in the structure of intermediate phase $BaCl_2.H_2O$ could also be monitored over the full temperature range for which it exists as a phase component with a level in excess of ~10% (~50 °C to 145 °C). Unlike the dihydrate, the expansion along the three crystallographic directions is approximately isotropic (see Figure 9), probably due to the fact that there are H…Cl bonds in all three axial directions (four longer H…Cl contacts in the bc plane and one much shorter and stronger H…Cl bond along *a* [21]). Of particular note is the potential in the present experiment to determine and monitor changes in hydrogen positions over this temperature range; these show some distinct trends. For example the H2 *x*-coordinate, plotted as a function of temperature in Figure 10 shows a gradual trend

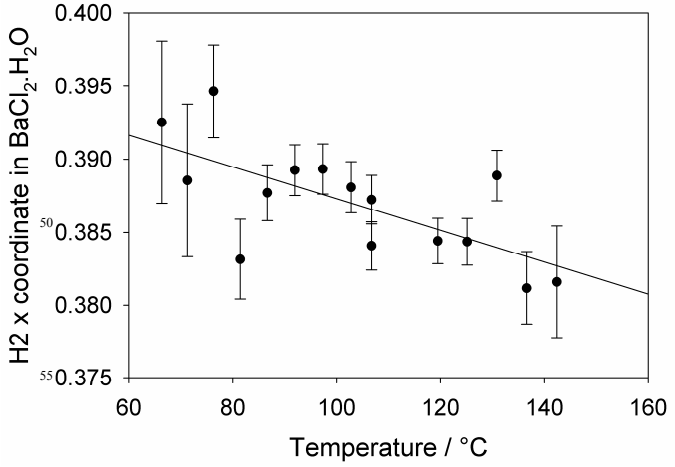

Figure 10. Variation of the H_2 *x* coordinate in $BaCl_2.H_2O$ with increased temperature, as refined from the five-minute NPD data sets. The straight line is a regression fit to the data; error bars are shown.

towards lower values as the decomposition temperature is approached, while the H1 *x* coordinate is increasing to a similar degree. This cooperative motion equates to tilting of the coordinated water molecule, which serves to create a more linear hydrogen bond between H1 and Cl2 as the temperature is increased. While great care should be taken in relating structural features to reaction processes, changes in such bonding patterns may allow a better understanding of the mechanism by which atoms and molecules start to rearrange themselves prior to a reaction.

Finally, over the highest temperature studied, the final dehydration product, anhydrous $BaCl_2$ is the dominant stable phase above ~150 °C. Its structure was monitored for a temperature range of only 20 °C and shows typical, uniform expansion rates along all three axes.

3.3. Rehydration of $BaCl_2$

In situ NPD data sets, collected during the dynamic hydration of a sample of anhydrous $BaCl_2$ at 298 K were used to extract the relative phase fractions for the anhydrous, monohydrate and dihydrate compounds as a function of hydration time, using the structures presented in Tables 1 – 3 as starting models. Figure 11 summarises the phase fraction of each phase in the sample over the 12 hr experiment. In principle such data can be used to investigate the kinetics of a reaction, as was recently demonstrated for the hydration of pharmaceutical excipients [26] . In this case, however, such analysis is highly complex, due to the presence of multiple phases in the system and uncontrolled diffusion kinetics of water vapour into the sample, and lies outside the scope of this article.

The anticipated complete conversion of the anhydrous $BaCl_2$, through pure monohydrate to the dihydrate phase was not achieved. Instead, over the majority of the experiment, there existed a three-phase mixture of the anhydrous, monohydrate (which reached a maximum phase fraction of ~60%) and dihydrate phases. This behaviour is at least in part due to experimental conditions, resulting from the combination of the very hygroscopic nature of the anhydrous starting material and the size of the sample can used, resulting in hydration gradients between the inside and outside of the cell. A further contributing factor may be that the kinetics of the hydration of the monohydrate are more rapid than those of the anhydrous material as might be expected if this phase forms as a coating on the anhydrous phase.

Sequential structure refinement against the 2.5 min data sets, while enabling identification of intermediate phases and the extraction of relative phase fractions of the three phases, was not useful for the extraction of accurate parametric data on the hydrogen atom positions for the monohydrate intermediate. This is because the ratio of refinable parameters to observations in a three phase mixture was too high, and the gradual and continuous nature of the change prevented binning of multiple sample sets.

In an attempt to obtain a diffraction pattern from the pure monohydrate intermediate, a stream of dry, <5% RH,

nitrogen gas was passed over the fully hydrated $BaCl_2.2H_2O$ sample at the conclusion of the initial hydration experiment. The background level of the NPD patterns (from the large incoherent scattering contribution of the hydrogen atoms and commensurate with the presence of water), showed a decrease consistent with loss of one water of crystallisation (*i.e.* dropping to ~50% of the background level of the dihydrate compound), reaching a plateau after the sample had converted completely to barium chloride monohydrate. There were no peaks pertaining to the dihydrate phase observable in the final diffraction pattern, and the dehydration did not proceed further to the anhydrous phase under these conditions. This approach allowed the compilation of several data sets to produce a longer data set with improved collection statistics, thus allowing more reliable crystallographic information on the structures to be extracted. The structure of the monohydrate could thus be freely refined with isotropic ADPs, resulting in a χ^2 value of 10.34 and an RF^2 of 6.93%. The structure refined for the monohydrate at RT corresponded well with that refined from the monohydrate data from the longer, compiled data set of the dehydration experiment above, at 110 ± 10 °C, having a refined O1_H1 distance of 0.901(2) O1_H2 distance of 0.990(18) Å, and H1_O1_H2 angle of 99.4 (9)°. The orientation of the water molecule once again favoured the model of a single bifurcated and one nearly linear hydrogen bond. Furthermore, the H1 *x* and H2 *x* coordinates (0.4035(15) and 0.3939(15), respectively), are very close to the values that would be obtained from extrapolation of the temperature dependent trends of these coordinates (in *e.g.* Figure 10) back to 298 K. These coordinates are consistent with a water molecule that is less tilted towards the Cl2 atoms at RT (compared to the high temperature structure) with an O-H1 –Cl2 angle of ~135° as opposed to an angle of ~142° at 110° C, indicating that the structure of the monohydrate adjusts such that the strongest hydrogen bond in the structure becomes more closely linear at higher temperatures. The extraction of refinable short data sets collected *in situ* would benefit from improved sample can geometry or from tailoring the RH level to control the speed and extent of the reaction.

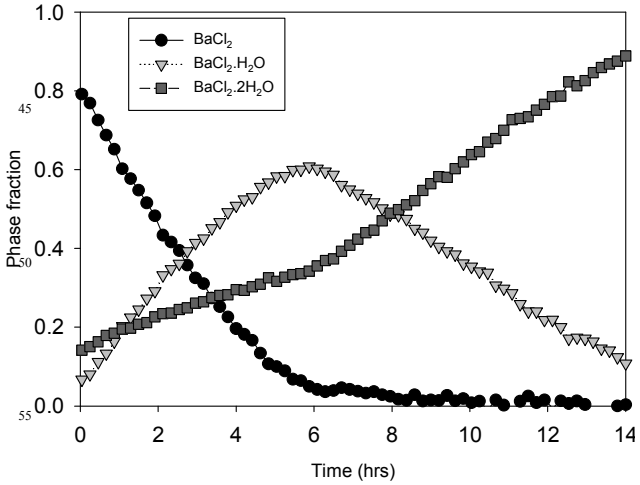

Figure 11. Phase fractions of the three $BaCl_2$ phases vs time exposed to a 100% RH gas flow, as refined from *in situ* hydration data.

4. Conclusions

Used at the most basic level the techniques used in this work can identify the presence and quantities of hydrogen-containing intermediates during thermal dehydration or controlled RH rehydration and in a bulk sample – rather than, as is often the case with X-ray powder diffraction methods, surface phases.

Analysis of the bulk phase fractions, determined from diffraction data, allows the investigation of the kinetics of a solid state reaction process [26]. As shown here, parametric NPD studies can be extended to full refinement of the structures of crystalline hydrogenous materials, and this provides a wealth of information on the changes occurring in material with changes in external conditions. These results highlight the quality of the structural information which can be obtained on the hydrogen positions in compounds containing coordinated water molecules from short NPD data collections under heating *in situ*. As the role of hydrogen bonding has been shown to impact on physical properties such as the rate of expansion of lattice parameters, further parametric investigations of the hydrogen positions in compounds will shed light on the origins of other behaviours, for example, favourable decomposition pathways. These methods may be applied widely to systems of import such as desiccants, building materials such as cements and plasters and also to pharma-compounds, while the amount and quality of information that can be extracted from such parametric experiments would be enhanced by the use of complementary parametric information such as DFT calculations, IR and NMR measurements [27].

In addition, the comparative study conducted here contrasts the type and quality of the information which can be extracted on hydration intermediates through use of *in situ* diffraction experiments. It was shown that controlled humidity experiments could provide a structural description of the intermediate that was consistent with the one achieved *via* dehydration, but at ambient temperatures. The RT rehydration and dehydration capability may therefore find application in the wetting and drying and cycling studies of commercial pharmaceuticals and excipients. In terms of isolating pure intermediate hydration products, in the case of very hygroscopic compounds, dehydration experiments, which afford tighter control on the activation temperatures for the dehydration steps, are more appropriate than *in situ* hydration, although development of the latter technique would open up the possibility of studying perhaps transient intermediate hydration products at ambient (rather than much elevated) temperatures.

This work was supported by EPSRC under grants EP/E051049 and EP/E050859. The authors thank Dr. Thomas Hansen for useful discussions, Dr. Jennifer Armstrong and Mr. Ben Littlefield for collection of some of the NPD data, and the Institut Laue-Langevin, Grenoble, for awards of beam time associated with proposals 5-25-167 and LTP-2-5A.

Notes and references

[a]*Department of Chemical Engineering, University of Bath, BATH, United Kingdom, E-mail: v.ting@bath.ac.uk*
[b]*European Spallation Source, LUND, Sweden*
University of Liverpool, LIVERPOOL, United Kingdom
[d]*Department of Chemistry, University of Bath, BATH, United KingdomSchool of Chemistry, University of Southampton, SOUTHAMPTON, United Kingdom, E-mail: mtw@soton.ac.uk*

1 M.C. Moron, *J. Mater. Chem.*, 2000, **10** 2617-2626.
2 O. Isnard, *J. Optoelectron. Adv. Mater.*, 2006, **8** 411-417.
3 J. Rodriguez, J.M. Gonzalezcalbet, J.C. Grenier, J. Pannetier, M. Anne, *Solid State Commun.*, 1987, **62** 231-234.
4 J.M. Rivas-Mercury, P. Pena, A.H. de Aza, X. Turrillas, *J. Eur. Ceram. Soc.*, 2008, **28** 1737-1748.
5 W. Abriel, K. Reisdorf, J. Pannetier, *Journal of Solid State Chemistry*, 1990, **85** 23-30.
6 C. Mellot-Draznieks, C. Serre, S. Surble, N. Audebrand, G. Ferey, *Journal of the American Chemical Society*, 2005, **127** 16273-16278.
7 T.A. Mary, J.S.O. Evans, T. Vogt, A.W. Sleight, *Science*, 1996, **272** 90-92.
8 G. Cruciani, G. Artioli, A. Gualtieri, K. Stahl, J.C. Hanson, *American Mineralogist*, 1997, **82** 729-739.
9 K. Stahl, in: R.M.E.J. Delhez (Ed.) 7th European Powder Diffraction Conference (EPDIC 7), Barcelona, Spain, 2000, pp. 346-350.
10 A.H. De Aza, M.A. Rodriguez, J.L. Rodriguez, S. De Aza, P. Pena, P. Convert, T. Hansen, X. Turrillas, *Journal of the American Ceramic Society*, 2002, **85** 881-888.
11 J.M.R. Mercury, P. Pena, A.H. de Aza, D. Sheptyakov, X. Turrillas, *Journal of the American Ceramic Society*, 2006, **89** 3728-3733.
12 R.W. Grimes, A.N. Fitch, *J. Mater. Chem.*, 1991, **1** 461-468.
13 K.D.M. Harris, R.L. Johnston, E.Y. Cheung, G.W. Turner, S. Habershon, D. Albesa-Jove, E. Tedesco, B.M. Kariuki, *Crystengcomm*, 2002, 356-367.
14 S. Hunig, K. Sinzger, M. Jopp, D. Bauer, W. Bietsch, J.U. Vonschutz, H.C. Wolf, *Angew. Chem.-Int. Edit.*, 1992, **31** 859-862.
15 S. Yevitz, *PCPDFWIN ref. 25-0610: β–Pt(NH$_3$)$_2$Cl$_2$.*
16 P.F. Henry, M.T. Weller, C.C. Wilson, *Submitted to Journal of Applied Crystallography*.
17 A. Oed, *Nuclear Instruments & Methods in Physics Research Section a-Accelerators Spectrometers Detectors and Associated Equipment*, 1988, **263** 351-359.
18 P.F. Henry, M.T. Weller, C.C. Wilson, *J. Appl. Crystallogr.*, 2009, **42** 1176-1188.
19 V.M. Padmanabhan, W.R. Busing, H.A. Levy, *Acta Crystallographica Section B*, 1978, **34** 2290-2292.
20 H.D. Lutz, W. Buchmeier, B. Engelen, *Acta Crystallographica Section B*, 1987, **43** 71-75.
21 H. Moller, T. Kellersohn, M. Schmidt, H.D. Lutz, J.K. Cockcroft, *Zeitschrift Fur Kristallographie*, 1993, **208** 19-26.
22 T.C. Hansen, P.F. Henry, H.E. Fischer, J. Torregrossa, P. Convert, in: 4th European Conference on Neutron Scattering, Iop Publishing Ltd, Lund, SWEDEN, 2007.
23 A.C. Larson, R.B.V. Dreele, *Los Alamos National Laboratory Report*, 1994, 86-748
24 B.H. Toby, *J. Appl. Cryst.*, 2001, **34** 210-213.
25 E.B. Brackett, T.E. Brackett, R.L. Sass, *The Journal of Physical Chemistry*, 1963, **67** 2132-2135.
26 S. Kirik, L. Solovyev, Blokhin, A, R. Mulagaleev, *PCPDFWIN ref. 50-0643: β–Pt(NH$_3$)$_2$Cl$_2$*, 1998.
27 M. Wiebcke, P. Sieger, J. Felsche, G. Engelhardt, P. Behrens, J. Schefer, *Zeitschrift für anorganische und allgemeine Chemie*, 1993, **619** 1321-1329.

